

INVESTIGATING THE IMPACT OF MODEL COMPLEXITY IN LARGE LANGUAGE MODELS

Jing Luo¹ Huiyuan Wang² Weiran Huang³

¹School of Mathematics and Statistics, Shandong University

²Perelman School of Medicine, University of Pennsylvania

³MIFA Lab, Qing Yuan Research Institute, SEIEE, Shanghai Jiao Tong University

ABSTRACT

Large Language Models (LLMs) based on the pre-trained fine-tuning paradigm have become pivotal in solving natural language processing tasks, consistently achieving state-of-the-art performance. Nevertheless, the theoretical understanding of how model complexity influences fine-tuning performance remains challenging and has not been well explored yet. In this paper, we focus on autoregressive LLMs and propose to employ Hidden Markov Models (HMMs) to model them. Based on the HMM modeling, we investigate the relationship between model complexity and the generalization capability in downstream tasks. Specifically, we consider a popular tuning paradigm for downstream tasks, head tuning, where all pre-trained parameters are frozen and only individual heads are trained atop pre-trained LLMs. Our theoretical analysis reveals that the risk initially increases and then decreases with rising model complexity, showcasing a “double descent” phenomenon. In this case, the initial “descent” is degenerate, signifying that the “sweet spot” where bias and variance are balanced occurs when the model size is zero. Obtaining the presented in this study conclusion confronts several challenges, primarily revolving around effectively modeling autoregressive LLMs and downstream tasks, as well as conducting a comprehensive risk analysis for multivariate regression. Our research is substantiated by experiments conducted on data generated from HMMs, which provided empirical support and alignment with our theoretical insights.

1 INTRODUCTION

Large Language Models (LLMs) have become a cornerstone in addressing a multitude of Natural Language Processing (NLP) tasks and have consistently demonstrated the state-of-the-art performance. Among the various approaches, the pre-trained fine-tuning paradigm stands out as the most prevalent and effective (Brown et al., 2020; Devlin et al., 2018), wherein fine-tuning involves training a fully connected network on a pre-trained LLM to tackle diverse downstream tasks. Recent research has underscored the significant impact of model complexity on the performance of fine-tuned LLMs (Nakkiran et al., 2019; Wei et al., 2023). However, the theoretical underpinnings of how model complexity influences fine-tuning performance remain unclear. In this paper, we delve into the intricate relationship between model complexity and the generalization capability of downstream tasks. We offer a theoretical analysis that elucidates the impact of increasing model size on the performance of LLMs. Our theoretical investigation aims to provide insights into the selection of an optimal model size to improve the performance of LLMs.

In practical applications, fine-tuning methods commonly involve adjusting the entire neural network (Devlin et al., 2018), and analyzing these methods theoretically can be challenging due to the intricate adjustments made to the parameters of pre-trained LLMs. However, a specific approach known as head tuning has garnered significant attention. Head tuning involves a scenario where all pre-trained parameters remain frozen, and only individual heads on top of the pre-trained LLMs are trained to enhance their performance on specific tasks. This methodology allows us to treat the pre-trained LLM as a black box (Peters et al., 2018). Although head tuning simplifies the process, it still adheres to the fundamental pre-trained fine-tuning paradigm. Moreover, in situations involving substantial distribution shifts, head tuning has demonstrated the potential to outperform

full fine-tuning (Kumar et al., 2022). Simultaneously, head tuning can be considered a form of representation learning, where we fine-tune a specific head on the representation of input tokens to address downstream tasks effectively. In summary, research on head tuning holds significant value and importance, attracting considerable interest from researchers (Wei et al., 2021; Saunshi et al., 2020).

While deep learning models like LLMs have showcased their formidable capabilities, our comprehension of their theoretical foundations remains somewhat limited. In previous studies exploring deep neural networks, there has been a tendency to simplify the analysis by considering single-layer linear settings (Huang et al., 2022; Saunshi et al., 2020; Wei et al., 2021; D’Ascoli et al., 2020). However, in the realm of deep learning, when we delve into what’s known as the “lazy regime” (Chizat et al., 2019), where neural network weights remain close to their initial values during training, the deep neural network can be effectively linearized around its initial weights. Furthermore, it’s important to note that under this regime, any transformer can be viewed as a Neural Tangent Kernel (NTK) (Yang, 2020). An NTK is approximately equivalent to a random feature model (Jacot et al., 2020), which is linear in its parameters. These observations suggest that linear approximations can effectively capture predictive characteristics, even when dealing with distinct model structures. Simultaneously, it’s important to note that although there have been numerous works investigating the relationship between model complexity and prediction risk under linear settings (Belkin et al., 2020; Hastie et al., 2022), their applicability to our research is limited. This limitation stems from the unique characteristics of LLMs in our analysis, particularly our consideration of the model as an autoregressive one. In this context, we employ a Hidden Markov Model (HMM) to capture the autoregressive nature of LLMs, which sets our study apart from previous linear settings.

The HMM has a rich history in NLP and has found widespread applications, such as text tagging (Merialdo, 1994), alignment (Vogel et al., 1996), and language modeling (Huang, 2011; Wei et al., 2021). When dealing with the inherent complexity and irregularities of real-world data, it is essential to recognize the need for simplification. In the context of next word prediction tasks, each word within our corpus is probabilistically linked to every preceding word, reflecting the inherent dependencies in language. In this setup, it is common to consider the input data as the hidden states in an HMM, with the representations of the input data serving as the observed states in the HMM. Considering the dependent structure in an HMM, our model can effectively capture essential representations of natural languages (Weikum, 2002; Chiu and Rush, 2020). Prior research has employed HMMs to investigate autoregressive models, demonstrating that head tuning can recover downstream labels (Wei et al., 2021). In contrast, our study focuses on establishing the next-word prediction risk and analyzing its relationship with model complexity. Additionally, there exist works that analyze regression errors in time series data without making the assumption of independence and identically distributed (i.i.d.) data generation processes (Lee and Lee, 2023). However, these studies do not incorporate the Hidden Markov assumption. Therefore, compared to their work, our research aligns more closely with NLP tasks, where the influence of sequential dependencies is crucial.

Specifically, our analysis assumes that we observe a sequence of tokens, which we employ to train an autoregressive LLM capable of predicting the next token. Subsequently, our downstream task revolves around learning a linear head to predict the next hidden state based on the predicted token. Our research commences with the establishment of our prediction risk, followed by a comprehensive bias-variance decomposition. To account for differences in the analysis, we divide our subsequent examination into two segments, focusing on the underparametrized case where the model size is smaller than the sample size and the overparametrized case where the model size is larger than the sample size, respectively. By combining insights from these two cases, we derive our estimate of the risk as a function of model complexity. Our findings reveal a phenomenon known as “double descent” (Belkin et al., 2019), wherein the LLM’s risk initially increases and then decreases with an increase in model complexity. Notably, the initial “descent” is degenerate, indicating that the point at which bias and variance are balanced, the “sweet spot” occurs when the model size is zero. Our primary contributions encompass the utilization of HMM to model autoregressive LLMs. We subsequently establish the next-word prediction risk and investigate its intricate relationship with model complexity. Additionally, we extend previous research on asymptotic risk in univariate regression to the realm of multiple regression. Under the assumptions we lay out, we provide an estimate for next-word prediction risk and offer practical suggestions for selecting an optimal model size.

RELATED WORK

Large language models. In the realm of theoretical analysis of autoregressive LLMs, an extensive body of work has emerged. For instance, in (Lee et al., 2021), the authors established that, under their specified assumptions, training a linear head on autoregressive LLMs enables the prediction of one observed variable from another. Additionally, the work in (Malladi et al., 2023) offers an explanation for the efficacy of parameter-efficient subspace-based fine-tuning methods for pre-trained language models, grounded in a kernel view. Furthermore, Saunshi et al. (2020) offers intuitive and mathematical explanations for the success of language model features in classification tasks by reinterpreting them as sentence completion problems.. Several other theoretical studies delve into the principles of self-supervised or contrastive learning, as evident in (Saunshi et al., 2019; HaoChen et al., 2021; Tosh et al., 2021a; Wei et al., 2020; Tosh et al., 2021b). Recent theoretical investigations have particularly focused on LLMs built upon the Transformer architecture, as exemplified by the prominent GPT series. For instance, in (Feng et al., 2023), an analysis was conducted to explore how Chain-of-Thought prompting enhances the performance of Transformer-based LLMs from a computational perspective. Furthermore, the authors of (Bai et al., 2023) made significant strides in enhancing our understanding of the formidable in-context learning capabilities exhibited by Transformer models. These theoretical studies collectively contribute to a deeper comprehension of the principles underlying the robustness and efficacy of LLMs in various NLP tasks.

Double descent. The double descent phenomenon was initially introduced by (Belkin et al., 2019) and subsequently observed in various contexts, including (Hastie et al., 2022; Advani et al., 2020; Spigler et al., 2018; Geiger et al., 2019). Notably, researchers have documented instances of the double descent phenomenon in the context of model size in Transformer architectures as well (Nakkiran et al., 2019). To date, there has been a significant body of work focused on the theoretical analysis of double descent. Some of these analyses have been performed in the setting of linear least squares regression (Belkin et al., 2020; Hastie et al., 2022; Bartlett et al., 2020; Muthukumar et al., 2020). In the context of adversarial training, Chen et al. (2020) identified and demonstrated the existence of the double descent phenomenon using Gaussian and Bernoulli models. Under the same adversarial training setting, Min et al. (2020) provided proof based on Gaussian models. Furthermore, Javanmard et al. (2020) revealed the occurrence of double descent in adversarially robust linear regression. Additionally, the authors of (Dar et al., 2020) demonstrated that the generalization errors in corresponding subspace fitting problems follow double descent trends as the settings become more supervised and less orthonormally constrained. In the domain of reinforcement learning, Fei et al. (2020) delved into the risk-sample tradeoff. However, the double descent phenomenon in deep learning still remains without a comprehensive explanation, as a theoretical proof for its occurrence has yet to be established by any researcher.

2 FORMULATIONS AND NOTATION

In our investigation, the modeling of the next word prediction task holds significant importance. When confronted with the inherent complexity and irregularities of real-world data, it becomes crucial to simplify our approach. Specifically, within the realm of next word prediction tasks, each word in our corpus exhibits probabilistic associations with every preceding word, thus capturing the inherent linguistic dependencies. When a word is encountered, the probability distribution of the subsequent word is primarily influenced by the current word. To streamline our analysis, we employ a simplifying assumption in which the input word follows a Markov chain distribution. Within this simplified framework, the probability of the next word is exclusively dependent on the preceding word. By considering the dependent structure inherent in an HMM, our model can effectively capture essential representations of natural languages. (Weikum, 2002; Chiu and Rush, 2020).

Data distribution. Define $z_i^{1 \times d} \in \{1, 2, \dots, H\}^d$ as the i th input token, which obeys the Markov chain distribution. First, we assume that $z_0 \sim N(0, I_d)$, where z_0 is the first token of the input sentence. Define $A \in \mathbb{R}^{d \times d}$ the transition matrix of z_i . Subsequently, we establish continuous forms to represent the distribution of z_i .

$$z_i = z_{i-1}A + \varepsilon_i, \quad \varepsilon_i \sim N(0, \sigma_\varepsilon^2 I_d).$$

It is important to highlight that in our context, A represents the transition matrix. When z_0 is established, our objective is to introduce randomness into the distribution of subsequent tokens to better align with real-world scenarios. To achieve this, we employ a continuous approach by incorporating noise to enhance the level of randomness. It is noteworthy that z_0 follows a normal distribution with a mean of zero and an identity covariance matrix, denoted as $N(0, I_d)$. Subsequently, each z_i is generated in accordance with a Markov Model. For any $0 \leq i \leq n$, z_i follows a normal distribution with a mean of zero and a covariance matrix represented as Σ_z , where

$$\Sigma_z = \sum_{j=1}^i (A^T)^j A^j + I.$$

Model setting. We assume that $x_i := (x_{i1}, \dots, x_{ip})$ is a representation of z_i , where z_i is the i th input token. To simplify our analysis, we assume that it is a linear representation, which satisfy

$$x_i = z_i W + u_i,$$

where $u_i := (u_{i1}, \dots, u_{ip})$ is a noisy, satisfying $u_{ij} \sim N(0, 1)$, and let $W \in \mathbb{R}^{d \times p}$ denote the representation matrix. Define target $y_i^{1 \times d} \in \{1, 2, \dots, H\}^d$ to be the next word of z_i , which satisfy

$$y_i = z_i A + \xi_i,$$

where $\xi_i \in \mathbb{R}$ is also a noisy, satisfying $\xi_i \sim N(0, \sigma_\xi^2)$. Then we have $x_i \sim N(0, \Sigma_x)$ and $y_i \sim N(0, \Sigma_y)$, where

$$\Sigma_y = A^T \left(\sum_{j=1}^i (A^T)^j A^j + I \right) A + \Sigma_\xi,$$

$$\Sigma_x = W^T \left(\sum_{j=1}^i (A^T)^j A^j + I \right) W + I.$$

When employing LLMs for next-word prediction, a common procedure involves feeding all word embeddings within a sentence into a pre-trained model to obtain their corresponding output representations. Subsequently, a feed-forward network is trained on the output representation of the last word, enabling the prediction of the subsequent word. In our framework, we assume the linearity of our pre-trained model, denoted as W , and we limit the feed-forward network to a single layer, denoted as $\hat{B} \in \mathbb{R}^{p \times d}$. Given a sequence of tokens denoted as z_0, z_1, \dots, z_n , we derive their respective representations x_0, x_1, \dots, x_n . Our primary objective is to predict the next word, denoted as y_n , based on the representation x_n through the training of a single-layer feed-forward network represented by \hat{B} .

Notation. We introduce the following notation for clarity in our discussion. We denote the dimension of the word embeddings as H . Consequently, we define $z_i^{1 \times d} \in 1, 2, \dots, H^d$ as the representation of the i -th input token, $y_i^{1 \times d} \in 1, 2, \dots, H^d$ as the subsequent word following z_i , and $x_i^{1 \times p}$ as the representation of z_i . Specifically, d signifies the dimensionality of vectors z and y , while p represents the dimensionality of vector x . We denote the sample size of x as n and define the overparametrization ratio $\gamma = p/n$. Let Σ_α represent the covariance matrix associated with variable α , where α can take on values such as x, y, z, ϵ , and ξ . Furthermore, we introduce M^+ to denote the Moore-Penrose inverse of the matrix M . We make the assumption that the input vector z adheres to a Markov chain distribution, and we introduce $A \in \mathbb{R}^{d \times d}$ to denote the transition matrix. Additionally, we employ the symbols W to represent the representation matrix and \hat{B} to signify a single-layer feed-forward network. We introduce the concepts of bias and variance within the context of next-word prediction risk and ridge regression risk. Specifically, we define $B_X(\hat{B}; B)$ to represent the bias in next-word prediction risk, while $V_X(\hat{B}; B)$ quantifies the variance. Furthermore, we provide asymptotic approximations for these measures denoted as $\mathcal{B}(\gamma, \Sigma_x)$ and $\mathcal{V}(\gamma, \Sigma_x)$. Expanding our discussion to encompass the ridge regression scenario, we introduce $B_X(\hat{B}_\lambda; B)$ as the bias associated with ridge regression risk and $V_X(\hat{B}_\lambda; B)$ as the corresponding variance. In this context, we also present asymptotic approximations, which are expressed as $\mathcal{B}(\lambda; \gamma, \Sigma_x)$ and $\mathcal{V}(\lambda; \gamma, \Sigma_x)$.

Remark. We want to emphasize that our research should not be viewed as a mere extension of the previous work (Hastie et al., 2022). Our approach differs significantly, as we assume that the data originates from a HMM, which moves beyond the basic i.i.d. framework used in the previous work. Furthermore, our analysis focuses on next-word prediction, which represents a progression from a univariate to a multivariate regression model. These aspects introduce significant challenges, particularly in analyzing asymptotic bias and variance, thereby distinguishing our work from the previous study (Hastie et al., 2022).

Moreover, our findings, which rely on linear models, have the potential to be extended to cases with a multi-layer head, such as transformers. This extension is viable because any transformer can be regarded as a NTK under the lazy regime (Yang, 2020), and an NTK is approximately equivalent to a random feature model (Jacot et al., 2020), which is linear in its parameters. Consequently, the use of linear approximation from embeddings to outputs is not an oversimplification but rather a widely recognized approach in the field, as evidenced by other studies (Wei et al., 2021).

3 ANALYSIS

In this section, we embark on an investigation into the risk associated with next-word prediction. Our analytical exploration comprises three key components. In the first part, we lay the foundational groundwork. Through a covariance alignment between the representation and the subsequent word, we refine our model. Following this, we introduce the concept of next-word prediction risk and provide a comprehensive bias-variance decomposition.

Notably, the behavior of the matrix $X^T X$ exhibits an invertible nature when the number of model size p is less than the sample size n , and it becomes singular when p exceeds n . Consequently, our analysis diverges into two distinct segments. In the second part, we delve into the scenario of underparametrization, where $p < n$. In the third part, we explore the overparametrized case, where $p > n$. Finally, we synthesize the insights gained from these two cases to formulate our ultimate conclusion.

3.1 FOUNDATIONAL PREPARATION

Recall the distribution of the i th input token z_i , z_i 's next word y_i and z_i 's representation x_i . Regress y_i on x_i , we can rewrite our model as

$$y_i = x_i B + \epsilon,$$

where

$$B = W^T \left(\sum_{j=1}^i (A^T)^j A^j + I \right) \left(I + W W^T \left(\sum_{j=1}^i (A^T)^j A^j + I \right) \right)^{-1} A, \quad \epsilon \sim N(0, \Sigma_\epsilon),$$

$$\Sigma_\epsilon = \Sigma_\xi + A^T \left(I + \left(\sum_{j=1}^i (A^T)^j A^j + I \right) W W^T \right)^{-1} \left(\sum_{j=1}^i (A^T)^j A^j + I \right) A.$$

In this step, we adopt an approach akin to that of (Hastie et al., 2022) by aligning the covariances between these variables. In this paper, we focus on training a single-layer feed-forward network on the output of pre-trained LLMs, which corresponds to the representation x_i . Consequently, we assume that the training process is effective, resulting in a training error of zero. Thus, we can regard our single-layer feed-forward network after training as a least squares estimator \hat{B} with n training cases, where:

$$\hat{B} = (X^T X)^+ X^T Y.$$

Here $X^{n \times p}$ is the representation matrix with rows x_i , and Y is the target matrix with rows y_i , where $0 \leq i \leq n - 1$. The notation $(X^T X)^+$ refers to the Moore-Penrose inverse of the matrix $X^T X$.

Consider a test sample (x_n, y_n) , for an estimator \widehat{B} , we define the out-of-sample next word prediction risk as

$$R_X(\widehat{B}; B) = E(\text{Tr}[(x_n B - x_n \widehat{B})^T (x_n B - x_n \widehat{B})]).$$

Also we have the bias-variance decomposition

$$\begin{aligned} R_X(\widehat{B}; B) &= E(\text{Tr}((x_n B - E(x_n \widehat{B}))^T (x_n B - E(x_n \widehat{B})))) \\ &\quad + E(\text{Tr}((E(x_n \widehat{B}) - x_n \widehat{B})^T (E(x_n \widehat{B}) - x_n \widehat{B}))). \end{aligned}$$

The conventional bias-variance decomposition historically applied to univariate regression. In contrast, our approach involves multiple regression, signifying a departure from past practices. Consequently, here we have extended the traditional bias-variance decomposition, originally designed for single regression, to encompass the realm of multiple regression.

3.2 UNDERPARAMETRIZED ASYMPTOTICS

In this subsection we first consider the underparametrized case, which means $p < n$. We consider an asymptotic setup that $n, p \rightarrow \infty$, and in such a way that $p/n \rightarrow \gamma$. To establish the subsequent theorem, we first present the following lemma, which is straightforward to demonstrate.

Lemma 1. *For the least squares estimator \widehat{B} , the next word prediction risk has bias defined as $B_X(\widehat{B}; B)$, and variance defined as $V_X(\widehat{B}; B)$.*

$$\begin{aligned} B_X(\widehat{B}; B) &= \text{Tr}(B^T (X^T X (X^T X)^+ - I) \Sigma_x ((X^T X)^+ X^T X - I) B), \\ V_X(\widehat{B}; B) &= \text{Tr}(\Sigma_\epsilon) \text{Tr}(\Sigma_x (X^T X)^+). \end{aligned}$$

Proof. Notice that $E(\widehat{B}) = (X^T X)^+ X^T X B$, and recall that $\widehat{B} = (X^T X)^+ X^T Y$, hence, it is straightforward to derive this lemma.

Under the underparameterized assumption, it is worth noting that $X^T X$ is invertible, and as evident from the aforementioned lemma, the bias effectively amounts to zero in this scenario. Given this observation and harking back to the bias-variance decomposition of the next word prediction risk, we can now state the following theorem.

Theorem 1. *Assume that $\lambda_{\min}(\Sigma_x) \geq c > 0$ for all n, p and a constant c , then as $n, p \rightarrow \infty$, in such a way that $p/n \rightarrow \gamma < 1$, the next word prediction risk satisfies, almost surely*

$$\lim_{n \rightarrow \infty} R_X(\widehat{B}; B) = \text{Tr}(\Sigma_\epsilon) \frac{\gamma}{1 - \gamma}.$$

We will complete the proof in Appendix A.

As an initial observation, it is important to highlight that in the underparametrized regime, where the ratio $\gamma < 1$, the minimum-norm estimator aligns with the conventional least squares estimator. In this scenario, the primary source of risk is attributed solely to variance, and there is no bias. Moreover, it is noteworthy that this risk does not exhibit any dependency on the parameters B and Σ_x . Interestingly, as we approach the interpolation boundary, where γ tends towards 1, the asymptotic risk experiences a significant increase.

It is worth noting that, as depicted in Figure 1, the risk curve of Theorem 1 in the underparameterized regime does not conform to the typical U-shaped pattern. It is essential to acknowledge that the U-shaped curve does not universally manifest, as discussed by (Chen et al., 2021). For instance, there is no U-shaped curve evident in Figure 1 of (Belkin et al., 2020). In practical applications, such as when employing Transformers for language translation (e.g., IWSLT'14 German-to-English) as documented in (Nakkiran et al., 2019), the classical U-shaped curve is notably absent. Simultaneously, the absence of the U-shaped curve was also observed in our own simulation experiments.

3.3 OVERPARAMETRIZED ASYMPTOTICS

In this subsection, we delve into the overparametrized scenario, where the presence of non-zero bias is notable. The next-word prediction risk is intricately tied to the geometric properties of Σ_x . To elucidate, we introduce the eigenvalues of Σ_x as s_1, s_2, \dots, s_p , where $s_1 \geq s_2 \geq \dots \geq s_p \geq 0$. Subsequently, we articulate our assumptions concerning our model, where M represents a substantial constant.

Assumption 1. Recall the eigenvalue of Σ_x and the overparametrization ratio $\gamma = p/n$, we have

- (1) $s_1 \leq M, \sum_{i=1}^p \frac{1}{s_i} \leq M$.
- (2) $|1 - p/n| \geq 1/M, 1/M \leq p/n \leq M$.

Assumption(1) necessitate that the eigenvalues of Σ_x exhibit bounded characteristics, while also avoiding accumulation in close proximity to zero. And assumption(2) mandates that the ratio of p to n remains within bounds, while also maintaining a separation from the critical threshold of interpolation, denoted by $p/n = 1$.

Definition 1. Define $\gamma = p/n$, for $\gamma \in \mathbb{R}_{>1}$, define c_0 to be the unique non-negative solution to

$$1 - \frac{1}{\gamma} = \sum_{i=1}^p \frac{1}{1 + c_0 \gamma s_i}. \quad (1)$$

When the value of γ exceeds one, the left-hand side of the equation mentioned above remains a constant within the range of zero to one. On the other hand, the function on the right-hand side displays monotonic behavior concerning the parameter c_0 . As c_0 approaches zero, the function value tends toward one, and as c_0 approaches infinity, the function value tends toward zero. This characteristic implies that the equation must possess a unique non-negative solution.

However, it's important to note that when the eigenvalue composition of Σ_x becomes complex, solving the analytical solution of the equation can become significantly challenging. In such cases, the solution may require advanced numerical methods or specialized techniques to obtain accurate results. And then we define the bias and variance of the next word prediction risk.

Definition 2. We define bias as $\mathcal{B}(\gamma, \Sigma_x)$ and variance as $\mathcal{V}(\gamma, \Sigma_x)$, as shown below

$$\begin{aligned} \mathcal{B}(\gamma, \Sigma_x) &:= \left\{ 1 + \gamma c_0 \frac{\sum_{i=1}^p \frac{s_i^2}{(1+c_0\gamma s_i)^2}}{\sum_{i=1}^p \frac{s_i}{(1+c_0\gamma s_i)^2}} \right\} \text{Tr}(B^T (I + c_0 \gamma \Sigma_x)^{-2} \Sigma_x B), \\ \mathcal{V}(\gamma, \Sigma_x) &:= \text{Tr}(\Sigma_x) \gamma c_0 \frac{\sum_{i=1}^p \frac{s_i^2}{(1+c_0\gamma s_i)^2}}{\sum_{i=1}^p \frac{s_i}{(1+c_0\gamma s_i)^2}}. \end{aligned}$$

It is worth noting that the most intricate aspect of numerically evaluating $\mathcal{B}(\gamma, \Sigma_x)$ and $\mathcal{V}(\gamma, \Sigma_x)$ lies in determining the unique non-negative solution of equation 1. The subsequent theorem establishes that, under appropriate technical conditions, the functions $\mathcal{B}(\gamma, \Sigma_x)$ and $\mathcal{V}(\gamma, \Sigma_x)$ play a pivotal role in characterizing the test error. It's worth noting that similar theorems in the context of univariate regression have been previously established in prior research (Hastie et al., 2022). We extend these findings to the domain of multiple regression.

Theorem 2. Assume that $\lambda_{\min}(\Sigma_x) > 1/M$, define $\gamma = p/n$, then for any constants $D > 0$ there exist $C = C(M, D)$, with probability at least $1 - Cn^{-D}$ the following hold

$$\begin{aligned} R_X(\hat{B}; B) &= B_X(\hat{B}; B) + V_X(\hat{B}; B), \\ |B_X(\hat{B}; B) - \mathcal{B}(\gamma, \Sigma_x)| &\leq C \frac{(\|B\|_F + 1)}{n^{1/4}}, \\ |V_X(\hat{B}; B) - \mathcal{V}(\gamma, \Sigma_x)| &\leq C \left(\frac{1}{n^{1/4}} + 1 \right). \end{aligned}$$

We prove this theorem in Appendix C.

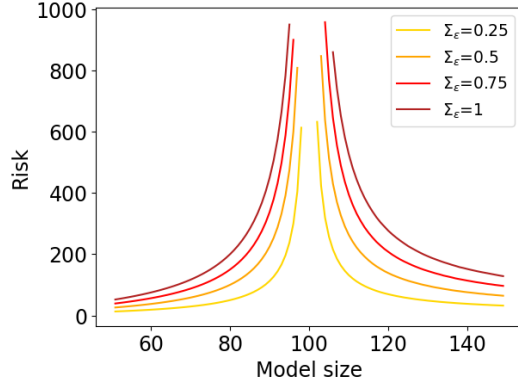


Figure 1: The risk curves illustrate the behavior of the least squares estimator \widehat{B} concerning its dependence on the model size, denoted as p , which is also the dimensionality of the vector x . In this context, p varies within the range of 50 to 150. These curves are based on a scenario with $n = 100$, $d = 50$, and varying levels of noise variance Σ_ϵ . The continuous lines represent the analytical predictions derived from Definition 2.

Theorem 2 establishes deterministic approximations for both bias and variance, which remain valid even for finite values of n and p , with $\gamma = p/n$ being a non-asymptotic quantity. Moreover, it's noteworthy that the error bounds demonstrated here display uniformity, signifying a pronounced dependence on the constant M . This characteristic sets it apart from the asymptotic context found in the works of (Richards et al., 2021; Wu and Xu, 2020).

To establish the proof of Theorem 2, we take an intermediate step by proving the following theorem within the context of ridge regression. In the case of ridge regression, under the same settings as those in the least squares estimator mentioned earlier, we introduce the ridge regression estimator denoted as \widehat{B}_λ . This estimator is computed as $\widehat{B}_\lambda = (X^T X + n\lambda I)^{-1} X^T Y$. It is essential to highlight that even though we consider our trained single-layer feed-forward network as a least squares estimator \widehat{B} , it can also be referred to as the “ridgeless” least squares estimator, due to the fact that $\widehat{B} = \lim_{\lambda \rightarrow 0^+} \widehat{B}_\lambda$. After completing the proof of Theorem 3, we will utilize this property of \widehat{B} to establish the proof of Theorem 2.

To facilitate our proof, we provide the subsequent definitions of bias and variance within the ridge regression framework.

Definition 3. For $\gamma \in \mathbb{R}_{>1}$ and $z \in \mathbb{C}_+$, where \mathbb{C}_+ represents the set of complex numbers with $\text{Im}(z) > 0$, we define $m_n(z)$ as the unique solution to the following equation

$$m_n(z) = \sum_{i=1}^p \frac{1}{[1 - \gamma - \gamma z m_n(z)] s_i - z}. \quad (2)$$

Additionally, we define $m_{n,1}(z)$ as follows

$$m_{n,1}(z) := \frac{\sum_{i=1}^p \frac{[1 - \gamma - \gamma z m_n(z)] s_i^2}{[(1 - \gamma - \gamma z m_n(z)) s_i - z]^2}}{1 - \gamma \sum_{i=1}^p \frac{z s_i}{[(1 - \gamma - \gamma z m_n(z)) s_i - z]^2}}. \quad (3)$$

We proceed to define the prediction bias of ridge regression as $\mathcal{B}(\lambda; \gamma, \Sigma_x)$ and the variance as $\mathcal{V}(\lambda; \gamma, \Sigma_x)$ through the following expressions

$$\begin{aligned} \mathcal{B}(\lambda; \gamma, \Sigma_x) &:= \lambda^2 (1 + \gamma m_{n,1}(-\lambda)) \text{Tr}(B^T (\lambda I + (1 - \gamma + \gamma \lambda m_n(-\lambda)) \Sigma_x)^{-2} \Sigma_x B), \\ \mathcal{V}(\lambda; \gamma, \Sigma_x) &:= \text{Tr}(\Sigma_\epsilon) \gamma \sum_{i=1}^p \frac{s_i^2 (1 - \gamma + \gamma \lambda^2 m_n'(-\lambda))}{[\lambda + s_i (1 - \gamma + \gamma \lambda m_n(-\lambda))]^2}. \end{aligned}$$

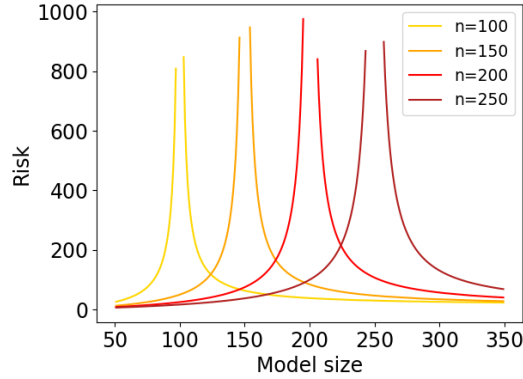


Figure 2: The risk curves illustrate the behavior of the least squares estimator \widehat{B} concerning its dependence on the model size, denoted as p , which is also the dimensionality of the vector x . In this context, p varies within the range of 50 to 350. These curves are based on a scenario with $\Sigma_\epsilon = 0.5$, $d = 50$, and varying levels of data samples n . The continuous lines represent the analytical predictions derived from Definition 2.

Next, we present our deterministic approximation of the prediction risk associated with ridge regression.

Theorem 3. *Assuming that Assumption 1 is satisfied, and given that $\lambda_{\min}(\Sigma_x) > 1/M$, we define $\gamma = p/n$. For any constants $D > 0$ (which can be arbitrarily large) and any $\epsilon > 0$ (which can be arbitrarily small), there exists a constant $C = C(M, D)$ such that, with a probability of at least $1 - Cn^{-D}$, the following conditions are met:*

$$\begin{aligned} R_X(\widehat{B}_\lambda; B) &= B_X(\widehat{B}_\lambda; B) + V_X(\widehat{B}_\lambda; B), \\ |B_X(\widehat{B}_\lambda; B) - \mathcal{B}(\lambda; \gamma, \Sigma_x)| &\leq \frac{C\|B\|_F}{n^{(1-\epsilon)/2}} \lambda, \\ |V_X(\widehat{B}_\lambda; B) - \mathcal{V}(\lambda; \gamma, \Sigma_x)| &\leq \frac{C}{\lambda^2 n^{(1-\epsilon)/2}}. \end{aligned}$$

The proof of this theorem is deferred to Appendix B.

Specifically, Theorem 3 provides non-asymptotic deterministic approximations for the ridge regression prediction bias $B_X(\widehat{B}_\lambda; B)$ and variance $V_X(\widehat{B}_\lambda; B)$. Notably, the error terms in these approximations exhibit uniformity with respect to the covariance matrix Σ_x and display a near-optimal dependence on the sample size n . Having established Theorem 3, we can now utilize it as a stepping stone to demonstrate the preceding Theorem 2.

Remark. By combining the insights from Theorem 1 and Theorem 2, we arrive at our estimation of the next-word prediction risk, as illustrated in Figure 1. It becomes evident that as the model size p increases, the risk exhibits a notable increase, particularly in proximity to the interpolation threshold $p/n = 1$. However, when the model size surpasses the number of input samples ($p > n$), we observe a subsequent decrease in risk. Notably, when the volume of input samples denoted by n expands, there is a corresponding requirement for the model size p to increase in order to reach the interpolation threshold. This phenomenon leads to a displacement of the threshold point towards the right, as visualized in Figure 2. These findings elucidate the underlying reasons for the occurrence of double descent behavior during the task of next-word prediction by LLMs and elucidate how augmenting the number of samples leads to a rightward shift in the peak of the test error, as previously discussed in Nakkiran et al. (2019).

In fact, our theory could still hold when the HMM assumption is relaxed. For instance, one can relax the Markov assumption in HMMs, where $z_i = z_{i-1}A + \epsilon$, into the case of more extended dependencies, such as $z_i = (z_{i-1}, \dots, z_{i-k})A + \epsilon$, where k is a fixed positive integer. Upon a careful review of our proof, we have found that our main results remain essentially the same with this

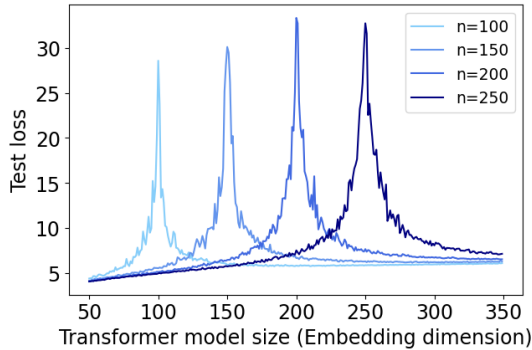


Figure 3: The cross-entropy test loss curve is generated by employing prediction through head tuning on the Transformer model. In this experiment, both the training and test data are generated using HMM.

adjustment. The primary difference is an increase in the number of columns, now adjusted to kd . We will consider other popular extensions of HMMs, such as auto-regressive HMM capturing long-term dependencies (Guan et al., 2016), as future work.

In light of our theoretical findings, we offer practical guidance on optimizing the trade-off between model size and training data volume. Our theoretical analysis indicates that the prediction error is minimized when the parameter count p is smaller than the number of training data samples n . Consequently, we advocate that for enhanced performance when employing LLMs to tackle downstream NLP tasks, the volume of training data should significantly surpass the model size. Indeed, this recommendation aligns with the empirical findings presented in Hoffmann et al. (2022) and is reflective of the emerging trend in the utilization of LLMs, as evidenced by recent work in the field (Touvron et al., 2023).

4 SIMULATION

In the preceding section, we established that the implementation of head tuning on pre-trained LLMs leads to a double descent phenomenon with the initial “descent” being degenerate. In the subsequent section, we aim to empirically validate our theoretical findings by applying head tuning to an encoder-decoder Transformer model using data generated by a HMM. Our objective is to corroborate our theoretical conclusions within a more practical and intricate context, where the representation of input tokens is acquired through a Transformer.

Training data and downstream task. In our experimental setup, we make an initial assumption that the first token, denoted as z_0 , follows a standard normal distribution with a mean of zero and an identity covariance matrix, represented as $N(0, I_d)$. Subsequently, we employ a HMM for generating the succeeding tokens. The transition matrix of the HMM is initialized randomly. Notably, we restrict our input to a single token at a time, and the primary objective of the downstream task is to predict the subsequent token based on the provided input token. Throughout our experiments, we will adjust the size of the hidden state within the HMM in the range of 50 to 150, in alignment with changes in the hidden dimension of the Transformer model.

Model training. Our approach to tackling downstream tasks involves conducting head tuning using an encoder-decoder Transformer architecture. In our experimental setup, we employ Transformer models with specific configurations: $model\ depths = 1$, $heads = 1$, and hidden size varies within the range of 50 to 350. Initially, we initialize the parameters of the Transformer randomly and maintain them as fixed, treating the Transformer as a pre-trained model. Subsequently, we train a single-layer feed-forward network using the representations generated by the Transformer to predict the subsequent token. To investigate the influence of model size, we systematically augment the Transformer’s capacity by increasing its hidden size. This augmentation is carried out incrementally, alongside corresponding adjustments to the hidden state size of the HMM. Notably, for each unique

combination of hidden size and hidden state size, we conduct separate training. Each test dataset includes $n_{test} = 20$ samples. To better support our theoretical conclusions, we selected four different numbers of training samples n_{train} : 100, 150, 200, and 250. We evaluate the model’s performance using the cross-entropy loss as the metric.

Results. Figure 3 illustrates our experimental findings, which reveal a notable trend: as the size of the Transformer model increases, the test error initially rises before subsequently declining. This observed pattern closely aligns with the conclusions drawn from our theoretical analysis. Additionally, it is noteworthy that the test loss is minimized when the Transformer model size is smaller than the number of training data samples, which further aligns with the conclusions drawn from our theoretical analysis.

5 CONCLUSION

In conclusion, our study delves into the intricate relationship between model complexity and fine-tuning performance in autoregressive LLMs. By employing HMMs to analyze autoregressive LLMs, we uncover a striking “double descent” pattern. This finding highlights the intricate interplay of model intricacy and generalization capacity in downstream tasks, particularly in the context of head tuning.

Nonetheless, our study comes with certain limitations. We restricted our investigation to a linear setting, which is a simplified approximation and may not fully capture the complexities of actual LLMs. Additionally, our analysis did not encompass prompt tuning, a highly effective fine-tuning technique that has garnered significant attention within the field. Extending our findings to address these limitations would be a valuable direction for future research.

REFERENCES

- Advani, M. S., Saxe, A. M., and Sompolinsky, H. (2020). High-dimensional dynamics of generalization error in neural networks. *Neural Networks*, 132:428–446.
- Bai, Y., Chen, F., Wang, H., Xiong, C., and Mei, S. (2023). Transformers as statisticians: Provable in-context learning with in-context algorithm selection.
- Bartlett, P. L., Long, P. M., Lugosi, G., and Tsigler, A. (2020). Benign overfitting in linear regression. *Proceedings of the National Academy of Sciences*, 117(48):30063–30070.
- Belkin, M., Hsu, D., Ma, S., and Mandal, S. (2019). Reconciling modern machine-learning practice and the classical bias–variance trade-off. *Proceedings of the National Academy of Sciences*, 116(32):15849–15854.
- Belkin, M., Hsu, D., and Xu, J. (2020). Two models of double descent for weak features. *SIAM Journal on Mathematics of Data Science*, 2(4):1167–1180.
- Brown, T., Mann, B., Ryder, N., Subbiah, M., Kaplan, J. D., Dhariwal, P., Neelakantan, A., Shyam, P., Sastry, G., Askell, A., Agarwal, S., Herbert-Voss, A., Krueger, G., Henighan, T., Child, R., Ramesh, A., Ziegler, D., Wu, J., Winter, C., Hesse, C., Chen, M., Sigler, E., Litwin, M., Gray, S., Chess, B., Clark, J., Berner, C., McCandlish, S., Radford, A., Sutskever, I., and Amodei, D. (2020). Language models are few-shot learners. In Larochelle, H., Ranzato, M., Hadsell, R., Balcan, M., and Lin, H., editors, *Advances in Neural Information Processing Systems*, volume 33, pages 1877–1901. Curran Associates, Inc.
- Chen, L., Min, Y., Belkin, M., and Karbasi, A. (2021). Multiple descent: Design your own generalization curve. In Ranzato, M., Beygelzimer, A., Dauphin, Y., Liang, P., and Vaughan, J. W., editors, *Advances in Neural Information Processing Systems*, volume 34, pages 8898–8912. Curran Associates, Inc.
- Chen, L., Min, Y., Zhang, M., and Karbasi, A. (2020). More data can expand the generalization gap between adversarially robust and standard models.
- Chiu, J. and Rush, A. (2020). Scaling hidden Markov language models. In Webber, B., Cohn, T., He, Y., and Liu, Y., editors, *Proceedings of the 2020 Conference on Empirical Methods in Natural Language Processing (EMNLP)*, pages 1341–1349, Online. Association for Computational Linguistics.
- Chizat, L., Oyallon, E., and Bach, F. (2019). On lazy training in differentiable programming. In Wallach, H., Larochelle, H., Beygelzimer, A., d’Alché-Buc, F., Fox, E., and Garnett, R., editors, *Advances in Neural Information Processing Systems*, volume 32. Curran Associates, Inc.
- Dar, Y., Mayer, P., Luzi, L., and Baraniuk, R. G. (2020). Subspace fitting meets regression: The effects of supervision and orthonormality constraints on double descent of generalization errors.
- D’Ascoli, S., Refinetti, M., Biroli, G., and Krzakala, F. (2020). Double trouble in double descent: Bias and variance(s) in the lazy regime. In III, H. D. and Singh, A., editors, *Proceedings of the 37th International Conference on Machine Learning*, volume 119 of *Proceedings of Machine Learning Research*, pages 2280–2290. PMLR.
- Devlin, J., Chang, M., Lee, K., and Toutanova, K. (2018). BERT: pre-training of deep bidirectional transformers for language understanding. *CoRR*, abs/1810.04805.
- Fei, Y., Yang, Z., Chen, Y., Wang, Z., and Xie, Q. (2020). Risk-sensitive reinforcement learning: Near-optimal risk-sample tradeoff in regret. In Larochelle, H., Ranzato, M., Hadsell, R., Balcan, M., and Lin, H., editors, *Advances in Neural Information Processing Systems*, volume 33, pages 22384–22395. Curran Associates, Inc.
- Feng, G., Zhang, B., Gu, Y., Ye, H., He, D., and Wang, L. (2023). Towards revealing the mystery behind chain of thought: A theoretical perspective.
- Geiger, M., Spigler, S., d’Ascoli, S., Sagun, L., Baity-Jesi, M., Biroli, G., and Wyart, M. (2019). Jamming transition as a paradigm to understand the loss landscape of deep neural networks. *Phys. Rev. E*, 100:012115.

- Guan, X., Raich, R., and Wong, W.-K. (2016). Efficient multi-instance learning for activity recognition from time series data using an auto-regressive hidden markov model. In Balcan, M. F. and Weinberger, K. Q., editors, *Proceedings of The 33rd International Conference on Machine Learning*, volume 48 of *Proceedings of Machine Learning Research*, pages 2330–2339, New York, New York, USA. PMLR.
- HaoChen, J. Z., Wei, C., Gaidon, A., and Ma, T. (2021). Provable guarantees for self-supervised deep learning with spectral contrastive loss. In Ranzato, M., Beygelzimer, A., Dauphin, Y., Liang, P., and Vaughan, J. W., editors, *Advances in Neural Information Processing Systems*, volume 34, pages 5000–5011. Curran Associates, Inc.
- Hastie, T., Montanari, A., Rosset, S., and Tibshirani, R. J. (2022). Surprises in high-dimensional ridgeless least squares interpolation. *The Annals of Statistics*, 50(2):949 – 986.
- Hoffmann, J., Borgeaud, S., Mensch, A., Buchatskaya, E., Cai, T., Rutherford, E., de Las Casas, D., Hendricks, L. A., Welbl, J., Clark, A., Hennigan, T., Noland, E., Millican, K., van den Driessche, G., Damoc, B., Guy, A., Osindero, S., Simonyan, K., Elsen, E., Rae, J. W., Vinyals, O., and Sifre, L. (2022). Training compute-optimal large language models.
- Huang, Y., Lin, J., Zhou, C., Yang, H., and Huang, L. (2022). Modality competition: What makes joint training of multi-modal network fail in deep learning? (Provably). In Chaudhuri, K., Jegelka, S., Song, L., Szepesvari, C., Niu, G., and Sabato, S., editors, *Proceedings of the 39th International Conference on Machine Learning*, volume 162 of *Proceedings of Machine Learning Research*, pages 9226–9259. PMLR.
- Huang, Z. (2011). *Modeling dependencies in natural languages with latent variables*. University of Maryland, College Park.
- Jacot, A., Gabriel, F., and Hongler, C. (2020). Neural tangent kernel: Convergence and generalization in neural networks.
- Javanmard, A., Soltanolkotabi, M., and Hassani, H. (2020). Precise tradeoffs in adversarial training for linear regression.
- Kumar, A., Raghunathan, A., Jones, R., Ma, T., and Liang, P. (2022). Fine-tuning can distort pretrained features and underperform out-of-distribution.
- Lee, J. D., Lei, Q., Saunshi, N., and ZHUO, J. (2021). Predicting what you already know helps: Provable self-supervised learning. In Ranzato, M., Beygelzimer, A., Dauphin, Y., Liang, P., and Vaughan, J. W., editors, *Advances in Neural Information Processing Systems*, volume 34, pages 309–323. Curran Associates, Inc.
- Lee, S. and Lee, S. (2023). The mean squared error of the ridgeless least squares estimator under general assumptions on regression errors. *arXiv preprint arXiv:2305.12883*.
- Malladi, S., Wettig, A., Yu, D., Chen, D., and Arora, S. (2023). A kernel-based view of language model fine-tuning. In Krause, A., Brunskill, E., Cho, K., Engelhardt, B., Sabato, S., and Scarlett, J., editors, *Proceedings of the 40th International Conference on Machine Learning*, volume 202 of *Proceedings of Machine Learning Research*, pages 23610–23641. PMLR.
- Merialdo, B. (1994). Tagging English text with a probabilistic model. *Computational Linguistics*, 20(2):155–171.
- Min, Y., Chen, L., and Karbasi, A. (2020). The curious case of adversarially robust models: More data can help, double descend, or hurt generalization.
- Muthukumar, V., Vodrahalli, K., Subramanian, V., and Sahai, A. (2020). Harmless interpolation of noisy data in regression. *IEEE Journal on Selected Areas in Information Theory*, 1(1):67–83.
- Nakkiran, P., Kaplun, G., Bansal, Y., Yang, T., Barak, B., and Sutskever, I. (2019). Deep double descent: Where bigger models and more data hurt. *CoRR*, abs/1912.02292.
- Peters, M. E., Neumann, M., Iyyer, M., Gardner, M., Clark, C., Lee, K., and Zettlemoyer, L. (2018). Deep contextualized word representations. *CoRR*, abs/1802.05365.

- Richards, D., Mourtada, J., and Rosasco, L. (2021). Asymptotics of ridge (less) regression under general source condition.
- Saunshi, N., Malladi, S., and Arora, S. (2020). A mathematical exploration of why language models help solve downstream tasks. *CoRR*, abs/2010.03648.
- Saunshi, N., Plevrakis, O., Arora, S., Khodak, M., and Khandeparkar, H. (2019). A theoretical analysis of contrastive unsupervised representation learning. In Chaudhuri, K. and Salakhutdinov, R., editors, *Proceedings of the 36th International Conference on Machine Learning*, volume 97 of *Proceedings of Machine Learning Research*, pages 5628–5637. PMLR.
- Spigler, S., Geiger, M., d’Ascoli, S., Sagun, L., Biroli, G., and Wyart, M. (2018). A jamming transition from under- to over-parametrization affects loss landscape and generalization. *CoRR*, abs/1810.09665.
- Tosh, C., Krishnamurthy, A., and Hsu, D. (2021a). Contrastive estimation reveals topic posterior information to linear models. *J. Mach. Learn. Res.*, 22(1).
- Tosh, C., Krishnamurthy, A., and Hsu, D. (2021b). Contrastive learning, multi-view redundancy, and linear models. In Feldman, V., Ligett, K., and Sabato, S., editors, *Proceedings of the 32nd International Conference on Algorithmic Learning Theory*, volume 132 of *Proceedings of Machine Learning Research*, pages 1179–1206. PMLR.
- Touvron, H., Lavril, T., Izacard, G., Martinet, X., Lachaux, M.-A., Lacroix, T., Rozière, B., Goyal, N., Hambro, E., Azhar, F., Rodriguez, A., Joulin, A., Grave, E., and Lample, G. (2023). Llama: Open and efficient foundation language models.
- Vogel, S., Ney, H., and Tillmann, C. (1996). Hmm-based word alignment in statistical translation. In *COLING 1996 Volume 2: The 16th International Conference on Computational Linguistics*.
- Wei, C., Shen, K., Chen, Y., and Ma, T. (2020). Theoretical analysis of self-training with deep networks on unlabeled data. *CoRR*, abs/2010.03622.
- Wei, C., Xie, S. M., and Ma, T. (2021). Why do pretrained language models help in downstream tasks? an analysis of head and prompt tuning. In Ranzato, M., Beygelzimer, A., Dauphin, Y., Liang, P., and Vaughan, J. W., editors, *Advances in Neural Information Processing Systems*, volume 34, pages 16158–16170. Curran Associates, Inc.
- Wei, J., Kim, N., Tay, Y., and Le, Q. V. (2023). Inverse scaling can become u-shaped.
- Weikum, G. (2002). Foundations of statistical natural language processing. *SIGMOD Rec.*, 31(3):37–38.
- Wu, D. and Xu, J. (2020). On the optimal weighted ℓ_2 regularization in overparameterized linear regression. In Larochelle, H., Ranzato, M., Hadsell, R., Balcan, M., and Lin, H., editors, *Advances in Neural Information Processing Systems*, volume 33, pages 10112–10123. Curran Associates, Inc.
- Yang, G. (2020). Tensor programs ii: Neural tangent kernel for any architecture.

Appendix

A PROOF OF THEOREM 1

Based on Lemma 1, it is evident that

$$\begin{aligned} B_X(\widehat{B}; B) &= \text{Tr}(B^T(X^T X(X^T X)^+ - I)\Sigma((X^T X)^+ X^T X - I)B) \\ &= 0. \end{aligned}$$

Simultaneously, it becomes apparent that

$$\begin{aligned} V_X(\widehat{B}; B) &= \text{Tr}(\Sigma_\epsilon)\text{Tr}(\Sigma(X^T X)^+ X^T X(X^T X)^+) \\ &= \text{Tr}(\Sigma_\epsilon)\text{Tr}(\Sigma(X^T X)^+) \\ &\rightarrow \text{Tr}(\Sigma_\epsilon)\frac{\gamma}{1-\gamma}. \end{aligned}$$

The final step can be derived from the proof of Proposition 2 presented in (Hastie et al., 2022). In summary, we can obtain

$$\lim_{n \rightarrow \infty} R_X(\widehat{B}; B) = \text{Tr}(\Sigma_\epsilon)\frac{\gamma}{1-\gamma}.$$

B PROOF OF THEOREM 3

As the proof of Theorem 2 relies on the foundation laid by Theorem 3, we will commence by presenting the proof of Theorem 3.

B.1 PROOF OF THEOREM 3: BIAS TERM

We will begin by providing a lemma that will serve as a useful tool for subsequent proofs.

Lemma 2. *For any square matrix $A^{p \times p}$ and matrix $B^{p \times d}$, there exists a vector $\beta^{p \times 1}$ such that $\|\beta\|_2 = \|B\|_F$, and this vector satisfies:*

$$\text{Tr}(B^T A B) \leq \beta^T A \beta.$$

Proof. Let

$$B = \begin{pmatrix} b_{11} & b_{12} & \cdots & b_{1d} \\ b_{21} & b_{22} & \cdots & b_{2d} \\ \vdots & \vdots & \ddots & \vdots \\ b_{p1} & b_{p2} & \cdots & b_{pd} \end{pmatrix},$$

$$\beta = (\beta_1, \beta_2, \cdots, \beta_p)^T,$$

and further let

$$A = \begin{pmatrix} a_{11} & a_{12} & \cdots & a_{1p} \\ a_{21} & a_{22} & \cdots & a_{2p} \\ \vdots & \vdots & \ddots & \vdots \\ a_{p1} & a_{p2} & \cdots & a_{pp} \end{pmatrix}.$$

Consequently, we can derive that

$$\beta^T A \beta = \sum_{i=1}^p \sum_{j=1}^p a_{ij} \beta_i \beta_j.$$

Moreover, we can also establish that

$$\begin{aligned}
\text{Tr}(B^T AB) &= \text{Tr}(ABB^T) \\
&= \text{Tr}\left(A \begin{pmatrix} \sum_{j=1}^d b_{1j}^2 & \sum_{j=1}^d b_{1j}b_{2j} & \cdots & \sum_{j=1}^d b_{1j}b_{pj} \\ \sum_{j=1}^d b_{2j}b_{1j} & \sum_{j=1}^d b_{2j}^2 & \cdots & \sum_{j=1}^d b_{2j}b_{pj} \\ \vdots & \vdots & \ddots & \vdots \\ \sum_{j=1}^d b_{pj}b_{1j} & \sum_{j=1}^d b_{pj}b_{2j} & \cdots & \sum_{j=1}^d b_{pj}^2 \end{pmatrix}\right) \\
&= \sum_{i=1}^p \sum_{j=1}^p a_{ij} \sum_{m=1}^d b_{jm}b_{im}.
\end{aligned}$$

If we assume that $\beta_i^2 = \sum_{j=1}^d b_{ij}^2$ for $i = 1, 2, \dots, p$, then it follows that $\|\beta\|_2 = \|B\|_F$. Subsequently, we can readily derive that

$$\sum_{m=1}^d b_{jm}b_{im} \leq \beta_i \beta_j, \quad 1 \leq i, j \leq p.$$

Hence, we can conclude that $\text{Tr}(B^T AB) \leq \beta^T A \beta$.

We will now commence with the proof of the bias term in Theorem 3. To begin, let's revisit the expressions for bias within our ridge regression framework at the regularization parameter λ :

$$B_X(\widehat{B}_\lambda; B) = \lambda^2 \text{Tr}(B^T (S_X + \lambda I)^{-1} \Sigma (S_X + \lambda I)^{-1} B).$$

Then we define

$$S_Z := \frac{Z^T Z}{n}, \quad S_X := \frac{X^T X}{n} = \Sigma^{1/2} S_Z \Sigma^{1/2}.$$

Building upon these expressions, we proceed to define

$$\begin{aligned}
\overline{F}_n(\eta, \lambda) &:= \text{Tr}(\lambda B^T (S_X + \lambda I + \lambda \eta \Sigma)^{-1} B) \\
&= \text{Tr}(\lambda B_\eta^T (\Sigma_\eta^{1/2} S_Z \Sigma_\eta^{1/2} + \lambda I)^{-1} B_\eta),
\end{aligned}$$

where

$$\Sigma_\eta := \Sigma(I + \eta \Sigma)^{-1}, \quad B_\eta := (I + \eta \Sigma)^{-1/2} B.$$

Then we can get

$$-\frac{\partial \overline{F}_n}{\partial \eta}(0, \lambda) = B_X(\widehat{B}_\lambda; B).$$

We define

$$F_n(\eta, \lambda) := -\text{Tr}(B_\eta^T (I + r_n(-\lambda, \eta) \Sigma \eta)^{-1} B_\eta),$$

where $r_n = r_n(-\lambda, \eta)$ represents the solution to the following equation:

$$\frac{1}{r_n} = \lambda + \gamma \frac{1}{p} \sum_{i=1}^p \frac{s_i(\eta)}{1 + s_i(\eta) r_n}.$$

Recalling the expression of the prediction bias as defined in Definition 3, it becomes evident that

$$-\frac{\partial F_n}{\partial \eta}(0, \lambda) = \mathcal{B}_X(\widehat{B}_\lambda; B).$$

We introduce the notation $s_1(\eta) \geq s_2(\eta) \geq s_3(\eta) \geq \dots \geq s_p(\eta)$ to represent the eigenvalues of Σ_η . Then, we define $r_n = r_n(z, \eta)$ as the unique solution of:

$$\frac{1}{r_n} = -z + \gamma \frac{1}{p} \sum_{i=1}^p \frac{s_i(\eta)}{1 + s_i(\eta)}.$$

By employing Lemma 2, It is straightforward to establish that there exists a vector β , where $\|\beta\|_2 = \|B\|_F$, and this β satisfies

$$\begin{aligned} \left| \frac{\partial \bar{F}_n}{\partial \eta}(0, \lambda) - \frac{\partial F_n}{\partial \eta}(0, \lambda) \right| &= |\lambda^2 \text{Tr}(B^T (S_X + \lambda I)^{-1} \Sigma (S_X + \lambda I)^{-1} B) \\ &\quad - \lambda^2 (1 + \gamma m_{n,1}(-\lambda)) \text{Tr}(B^T (\lambda I + (1 - \gamma + \gamma \lambda m_n(-\lambda)) \Sigma)^{-2} \Sigma B)| \\ &\leq |\lambda^2 \beta^T (S_X + \lambda I)^{-1} \Sigma (S_X + \lambda I)^{-1} \beta \\ &\quad - \lambda^2 (1 + \gamma m_{n,1}(-\lambda)) \beta^T (\lambda I + (1 - \gamma + \gamma \lambda m_n(-\lambda)) \Sigma)^{-2} \Sigma \beta| \\ &= \left| \frac{\partial(\lambda \beta_\eta^T (\Sigma_\eta^{1/2} S_Z \Sigma_\eta^{1/2} + \lambda I)^{-1} \beta_\eta)}{\partial \eta} \Big|_{\eta=0} - \frac{\partial(-\beta_\eta^T (I + r_n(-\lambda, \eta) \Sigma \eta)^{-1} \beta_\eta)}{\partial \eta} \Big|_{\eta=0} \right| \\ &\leq \frac{C \|B\|_F}{n^{(1-\epsilon)/2} \lambda}, \quad \forall \lambda \in (n^{-2/3+\epsilon_0}, \infty), \eta \in \left(-\frac{1}{2M}, \infty\right). \end{aligned}$$

The final step in this process can be derived from equation (85) in (Hastie et al., 2022). Note that

$$|B_X(\hat{B}_\lambda; B) - \mathcal{B}(\lambda; \gamma, \Sigma_x)| = \left| \frac{\partial \bar{F}_n}{\partial \eta}(0, \lambda) - \frac{\partial F_n}{\partial \eta}(0, \lambda) \right|,$$

thus, we have completed the proof of the bias term, and we will now proceed to prove the variance term.

B.2 PROOF OF THEOREM 3: VARIANCE TERM

To begin, let's also revisit the expressions for variance within our ridge regression framework at the regularization parameter λ :

$$\begin{aligned} V_X(\hat{B}_\lambda; B) &= \frac{\text{Tr}(\Sigma_\epsilon)}{n} \text{Tr}(\Sigma S_X (S_X + \lambda I)^{-2}) \\ &= \text{Tr}(\Sigma_\epsilon) \gamma \frac{\partial}{\partial \lambda} \left\{ \frac{\lambda}{p} \text{Tr}(\Sigma S_X (S_X + \lambda I)^{-2}) \right\}. \end{aligned}$$

We define

$$L_n(\lambda) := \frac{1}{p} \text{Tr}(\Sigma (I + r_n(-\lambda, 0) \Sigma)^{-1}).$$

Here, the r_n is defined as previously mentioned. From equation (85) in (Hastie et al., 2022), we can derive that

$$|V_X(\hat{B}_\lambda; B) - \text{Tr}(\Sigma_\epsilon) \gamma \frac{\partial L_n}{\partial \lambda}(\lambda)| \leq \frac{C}{\lambda^2 n^{(1-\epsilon)/2}}.$$

Here the second component within the absolute value represents the expression of the prediction variance $\mathcal{V}(\lambda; \gamma, \Sigma_x)$ as defined in Definition 3.

By combining the bias and variance terms, we have successfully completed the proof of Theorem 3. In the next stage, we will establish Theorem 2 based on the findings in Theorem 3.

C PROOF OF THEOREM 2

The proof is derived from Theorem 3, which approximates min-norm regression with ridge regression using a small value of λ . Therefore, for the purpose of this proof, we will assume that $\lambda \leq 1$.

C.1 PROOF OF THEOREM 2: BIAS TERM

Recalling the expressions $S_X := \frac{X^T X}{n}$ as defined in the proof of Theorem 3 and in Lemma 1, and once more leveraging the result from Lemma 2, it becomes evident that there exists a vector β , for which $\|\beta\|_2 = \|\widehat{B}\|_F$, and this β satisfies:

$$\begin{aligned} |B_X(\widehat{B}_\lambda; B) - B_X(\widehat{B}; B)| &= |\lambda^2 \text{Tr}(B^T (S_X + \lambda I)^{-1} \Sigma (S_X + \lambda I)^{-1} B) \\ &\quad - \text{Tr}(B^T (S_X S_X^+ - I) \Sigma (S_X^+ S_X - I) B)| \\ &\leq |\lambda^2 \text{Tr}(\beta^T (S_X + \lambda I)^{-1} \Sigma (S_X + \lambda I)^{-1} \beta) \\ &\quad - \text{Tr}(\beta^T (S_X S_X^+ - I) \Sigma (S_X^+ S_X - I) \beta)| \\ &\leq C(M)\lambda. \end{aligned}$$

The final step in this process can be derived from equation (104) in (Hastie et al., 2022). To enhance readability and comprehension, we introduce the following definitions

$$c_1 := c_0 \frac{\sum_{i=1}^p \frac{s_i^2}{(1+c_0\gamma s_i)^2}}{\sum_{i=1}^p \frac{s_i}{(1+c_0\gamma s_i)^2}}.$$

Taking into consideration the bias $\mathcal{B}(\gamma, \Sigma_x)$ defined in Definition 2 and the bias $\mathcal{B}(\lambda; \gamma, \Sigma_x)$ defined in Definition 3. By following the reasoning presented in the proof of the variance term in Section B.1 of (Hastie et al., 2022), we can ascertain that

$$\begin{aligned} m_n(-\lambda) &= (1 - \frac{1}{\gamma}) \frac{1}{\lambda} + c_0 + O(\lambda), \\ m_{n,1}(-\lambda) &= c_1 + O(\lambda). \end{aligned}$$

Then we can express that

$$\begin{aligned} |\mathcal{B}(\lambda; \gamma, \Sigma_x) - \mathcal{B}(\gamma, \Sigma_x)| &= |(1 + \gamma c_1) \text{Tr}(B^T (I + c_0 \gamma \Sigma)^{-2} \Sigma B) \\ &\quad - (1 + \gamma c_1 + \gamma O(\lambda)) \text{Tr}(B^T (I + c_0 \gamma \Sigma + \gamma O(\lambda) \Sigma)^{-2} \Sigma B)|. \end{aligned}$$

Let

$$f(x) = (1 + \gamma c_1 + x) \text{Tr}(B^T (I + c_0 \gamma \Sigma + x \Sigma)^{-2} \Sigma B).$$

Subsequently, in accordance with Lagrange's mean value theorem, there exists a value ξ in the interval $[0, x]$ such that

$$\frac{f(x) - f(0)}{x} = f'(\xi).$$

Thus, we can conclude that

$$\begin{aligned} |\mathcal{B}(\lambda; \gamma, \Sigma_x) - \mathcal{B}(\gamma, \Sigma_x)| &= |f(\gamma O(\lambda)) - f(0)| \\ &= |\{\text{Tr}(B^T (I + c_0 \gamma \Sigma + \xi \Sigma)^{-2} \Sigma B) \\ &\quad - 2(1 + \gamma c_1 + \xi) \text{Tr}(B^T (I + c_0 \gamma \Sigma + \xi \Sigma)^{-3} \Sigma B)\} \gamma O(\lambda)| \\ &\leq \{\text{Tr}(B^T (I + c_0 \gamma \Sigma + \xi \Sigma)^{-2} \Sigma B) \\ &\quad + 2(1 + \gamma c_1 + \xi) \text{Tr}(B^T (I + c_0 \gamma \Sigma + \xi \Sigma)^{-3} \Sigma B)\} \gamma O(\lambda) \\ &\leq C(M)\lambda. \end{aligned}$$

In summary, we can derive that

$$\begin{aligned} |B_X(\widehat{B}; B) - \mathcal{B}(\gamma, \Sigma_x)| &\leq |B_X(\widehat{B}_\lambda; B) - B_X(\widehat{B}; B)| + |\mathcal{B}(\lambda; \gamma, \Sigma_x) - \mathcal{B}(\gamma, \Sigma_x)| \\ &\quad + |B_X(\widehat{B}_\lambda; B) - \mathcal{B}(\lambda; \gamma, \Sigma_x)| \\ &= C(M)(\lambda + \frac{\|\widehat{B}\|_F}{n^{(1-\epsilon)/2}\lambda}). \end{aligned}$$

In this context, we set $\lambda = n^{-1/4}$ and select ϵ to be sufficiently small. Consequently, we can attain the desired bound as stipulated in Theorem 2.

C.2 PROOF OF THEOREM 2: VARIANCE TERM

We denote the eigenvalue decomposition of S_X as $S_X = UD_XU^T$, where $D_X \in \mathbb{R}^{p \times p}$ is a diagonal matrix, and $U \in \mathbb{R}^{p \times p}$ is an orthogonal matrix. Furthermore, we define $1_{D_X=0}$ as the diagonal matrix with the (i, i) -th entry equal to 1 if $(D_X)_{ii} = 0$ and equal to 0 otherwise. Subsequently, we can express the variance in Lemma 1 and the variance within our ridge regression framework as

$$\begin{aligned} V_X(\widehat{B}; B) &= \frac{\text{Tr}(\Sigma_\epsilon)}{n} \text{Tr}(\Sigma U D_X^{-1} 1_{D_X>0} U^T), \\ V_X(\widehat{B}_\lambda; B) &= \frac{\text{Tr}(\Sigma_\epsilon)}{n} \text{Tr}(\Sigma U D_X (\lambda I + D_X)^{-2} U^T). \end{aligned}$$

Then from (Hastie et al., 2022) we can derive that

$$|V_X(\widehat{B}_\lambda; B) - V_X(\widehat{B}; B)| \leq \frac{2\lambda M \text{Tr}(\Sigma_\epsilon)}{\sigma_{\min}(X)^4/n^2} \leq C(M)\lambda.$$

Taking into consideration the bias $\mathcal{V}(\gamma, \Sigma_x)$ defined in Definition 2 and the bias $\mathcal{V}(\lambda; \gamma, \Sigma_x)$ defined in Definition 3, we can express that

$$\begin{aligned} |\mathcal{V}(\lambda; \gamma, \Sigma_x) - \mathcal{V}(\gamma, \Sigma_x)| &= |\text{Tr}(\Sigma_\epsilon) \gamma \sum_{i=1}^p \frac{s_i^2(1 - \gamma + \gamma \lambda^2 m'_n(-\lambda))}{[\lambda + s_i(1 - \gamma + \gamma \lambda m_n(-\lambda))]^2} \\ &\quad - \text{Tr}(\Sigma_\epsilon) \gamma c_0 \frac{\sum_{i=1}^p \frac{s_i^2}{(1+c_0\gamma s_i)^2}}{\sum_{i=1}^p \frac{s_i}{(1+c_0\gamma s_i)^2}}|. \end{aligned}$$

Following the argument made in the proof of the variance term in Section B.1 of (Hastie et al., 2022), we can conclude that

$$|\mathcal{V}(\lambda; \gamma, \Sigma_x) - \mathcal{V}(\gamma, \Sigma_x)| \leq C(M)\lambda.$$

To sum up, we can derive that

$$\begin{aligned} |V_X(\widehat{B}; B) - \mathcal{V}(\gamma, \Sigma_x)| &\leq |V_X(\widehat{B}_\lambda; B) - V_X(\widehat{B}; B)| + |\mathcal{V}(\lambda; \gamma, \Sigma_x) - \mathcal{V}(\gamma, \Sigma_x)| \\ &\quad + |V_X(\widehat{B}_\lambda; B) - \mathcal{V}(\lambda; \gamma, \Sigma_x)| \\ &= C(M)\left(\lambda + \frac{1}{\lambda^2 n^{(1-\epsilon)/2}}\right). \end{aligned}$$

In this context, we also set $\lambda = n^{-1/4}$ and select ϵ to be sufficiently small. Consequently, we can attain the desired bound as stipulated in Theorem 2.

By merging the bias term and the variance term, we have successfully concluded the proof of Theorem 2.